pharmaceuticals

MDPI

Article

Selection of an Optimal Metabolic Model for Accurately Predicting the Hepatic Clearance of Albumin-Binding-Sensitive Drugs

Ren-Jong Liang [1,2], Shu-Hao Hsu [3], Hsueh-Tien Chen [3], Wan-Han Chen [3], Han-Yu Fu [3,4], Hsin-Ying Chen [5], Hong-Jaan Wang [2,3,5,*,†] and Sung-Ling Tang [2,3,4,5,*,†]

1 Clinical Pharmacy Department, Tri-Service General Hospital Keelung Branch, Keelung City 202006, Taiwan; 810010009@mail.ndmctsgh.edu.tw
2 Graduate Institute of Medical Sciences, National Defense Medical Center, Taipei 114201, Taiwan
3 School of Pharmacy, National Defense Medical Center, Taipei 114201, Taiwan; hsu.shuhao@mail.ndmctsgh.edu.tw (S.-H.H.); ccjh097429@gmail.com (H.-T.C.)
4 Department of Pharmacy Practice, Tri-Service General Hospital, Taipei 114202, Taiwan
5 Graduate Institute of Life Science, National Defense Medical Center, Taipei 114201, Taiwan
* Correspondence: hongjaan@mail.ndmctsgh.edu.tw (H.-J.W.); tangling@mail.ndmctsgh.edu.tw (S.-L.T.); Tel.: +886-2-8792-3100 (ext. 18849) (H.-J.W. & S.-L.T.)
† These authors contributed equally to this work.

Abstract

Background/Objectives: Hepatic clearance is important in determining clinical drug administration strategies. Achieving accurate hepatic clearance predictions through in vitro-to-in vivo extrapolation (IVIVE) relies on appropriate model selection, which is a critical step. Although numerous models have been developed to estimate drug dosage, some may fail to predict liver drug clearance owing to inappropriate hepatic clearance models during IVIVE. To address this limitation, an in silico-based model selection approach for optimizing hepatic clearance predictions was introduced in a previous study. The current study extends this strategy by verifying the accuracy of the selected models using ex situ experimental data, particularly for drugs whose model choices are influenced by protein binding. **Methods**: Commonly prescribed drugs were classified according to their hepatic extraction ratios and protein-binding properties. Building on previous studies that employed multinomial logistic regression analysis for model selection, a three-phase classification method was implemented to identify five representative drugs: diazepam, diclofenac, rosuvastatin, fluoxetine, and tolbutamide. Subsequently, an isolated perfused rat liver (IPRL) system was used to evaluate the accuracy of the in silico method. **Results**: As the unbound fraction increased for diazepam and diclofenac, the most suitable predictive model shifted from the initially preferred well-stirred model (WSM) to the modified well-stirred model (MWSM). For rosuvastatin, the MWSM provided a more accurate prediction. These three capacity-limited, binding-sensitive drugs conformed to the outcomes predicted by the multinomial logistic regression analysis. Fluoxetine was best described by the WSM, which is consistent with its flow-limited classification. For tolbutamide, a representative capacity-limited, binding-insensitive drug, no significant differences were observed among the various models. **Conclusions**: These findings demonstrate the accuracy of an in silico-based model selection approach for predicting liver metabolism and highlight its potential for guiding dosage adjustments. Furthermore, the IPRL system serves as a practical tool for validating the accuracy of the results derived from this approach.

check for updates

Academic Editor: Donato Colangelo

Received: 23 May 2025
Revised: 26 June 2025
Accepted: 29 June 2025
Published: 1 July 2025

Citation: Liang, R.-J.; Hsu, S.-H.; Chen, H.-T.; Chen, W.-H.; Fu, H.-Y.; Chen, H.-Y.; Wang, H.-J.; Tang, S.-L. Selection of an Optimal Metabolic Model for Accurately Predicting the Hepatic Clearance of Albumin-Binding-Sensitive Drugs. *Pharmaceuticals* **2025**, *18*, 991. https://doi.org/10.3390/ph18070991

Copyright: © 2025 by the authors. Licensee MDPI, Basel, Switzerland. This article is an open access article distributed under the terms and conditions of the Creative Commons Attribution (CC BY) license (https://creativecommons.org/licenses/by/4.0/).

Keywords: hepatic clearance; in vitro-to-in vivo extrapolation (IVIVE); isolated perfused rat liver (IPRL); well-stirred model (WSM); modified well-stirred model (MWSM); protein binding

1. Introduction

The liver is the primary organ involved in drug metabolism in humans. Since 1972, hepatic clearance (CL_H) has been widely studied and increasingly used in clinical practice [1]. One method for accurate CL_H predictions is in vitro-to-in vivo extrapolation (IVIVE), which eliminates the need for extensive animal experiments [2]. However, the accuracy of IVIVE relies on appropriate model selection, which is a critical step in the IVIVE process. Numerous models have been developed to predict hepatic drug metabolism [3–13]. Among these models, the well-stirred [7], parallel-tube [14], and dispersion [15] models (WSM, PTM, and DM, respectively) are commonly used to estimate CL_H. However, these models sometimes fail to evaluate drug metabolism accurately, leading to suboptimal therapeutic outcomes or toxicity. Previous investigations have shown that the traditional WSM (Equation (1), CL_H represents the hepatic clearance, Q_H is the hepatic blood flow, f_u is the unbound fraction in plasma, and CL_{int} is the intrinsic clearance of the drug) may not reliably predict the metabolic profiles of albumin-binding-sensitive drugs. In 2021, a refined version of the WSM, referred to as the modified WSM (MWSM; Equation (2)), was introduced to provide a more precise and comprehensive assessment of drug metabolism under defined conditions [6].

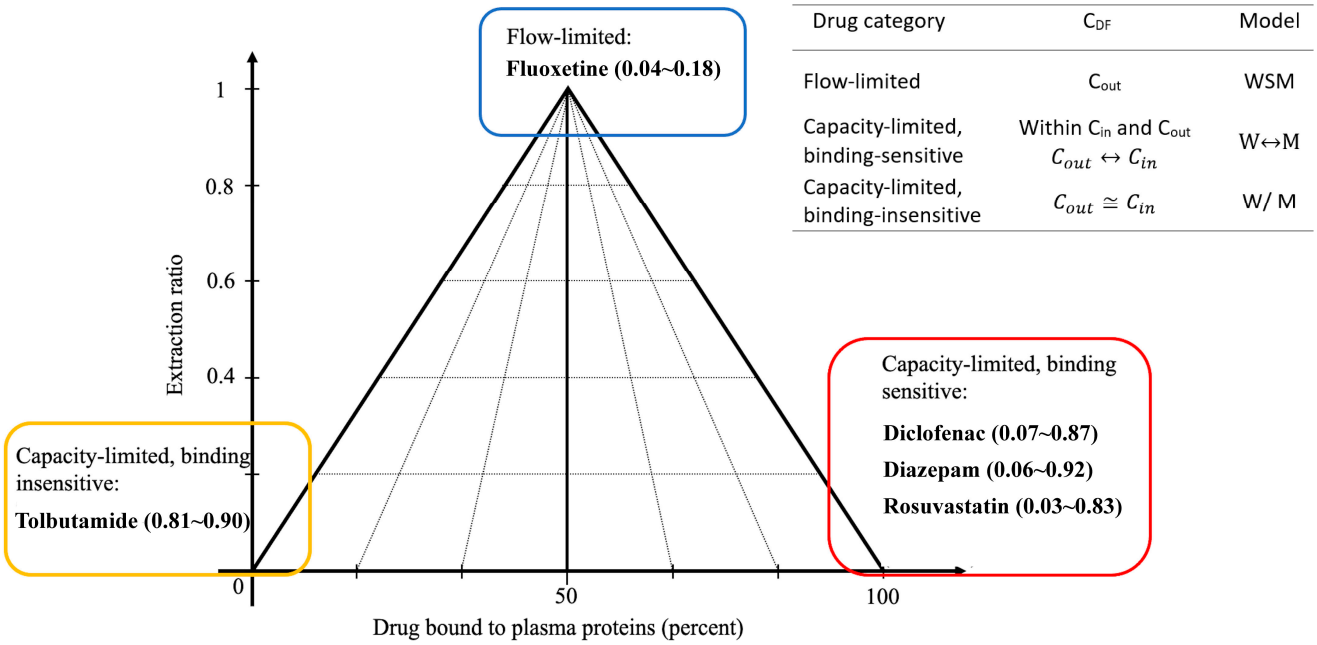
$$CL_H = \frac{Q_H \times f_u \cdot CL_{int}}{Q_H + f_u \cdot CL_{int}} \quad (1)$$

$$CL_H = f_u \cdot CL_{int} \quad (2)$$

Building on the principles of IVIVE, we previously established a categorized approach using in silico analysis to guide the selection of drug clearance models. This approach was developed based on 16 detailed physicochemical and pharmacokinetic parameters from 223 compounds and was derived through multinomial logistic regression analysis [3]. In the present study, to validate the predictive accuracy of this approach, we used it to determine the optimal CL_H model for three representative drugs: diazepam, diclofenac, and rosuvastatin. Each drug was classified according to one of the following three outcomes: W (better prediction with WSM), M (better prediction with MWSM), or S (equally accurate prediction with both models). The probabilities for each outcome were calculated, and the category with the highest probability was further verified by ex situ results obtained from liver perfusion experiments. This framework provides a robust data-driven methodology for determining the most suitable hepatic model based on drug-specific profiles, offering a systematic and optimized approach for enhancing the accuracy of IVIVE predictions.

In this study, the aforementioned strategy was experimentally validated. First, a widely used three-phase classification scheme was employed to identify the representative drugs from each category [16]. According to established pharmacokinetic concepts [8], flow-limited drugs (Figure 1, upper apex of the triangle) generally align with the "WSM recommended" category, whereas capacity-limited, binding-insensitive drugs (Figure 1, lower left of the triangle) tend to show "no significant difference across models." However, capacity-limited binding-sensitive drugs (Figure 1, lower right) represent more complex situations. For instance, a previous report [6] indicated that diazepam cannot always be described using a single model under varying protein concentrations. Therefore, a previously established in silico-based method was employed in the study to predict the optimal CL_H model for such drugs. These compounds were then subjected to isolated

perfused rat liver (IPRL) experiments with different protein concentrations to measure the CL_H. The resulting data verified the accuracy of the model selection by in silico analysis and provided a basis for further discussion of the drug–protein-binding effect.



Drug category	C_{DF}	Model
Flow-limited	C_{out}	WSM
Capacity-limited, binding-sensitive	Within C_{in} and C_{out} $C_{out} \leftrightarrow C_{in}$	W↔M
Capacity-limited, binding-insensitive	$C_{out} \cong C_{in}$	W/ M

Figure 1. Three-phase classification is based on different degrees of liver extraction ratio and plasma protein binding. The numbers in parentheses represent the range of liver bioavailability, as the protein concentration is adjusted. WSM or W: well-stirred model; M: modified well-stirred model; C_{DF}: driving force concentrations; C_{in}: drug concentration entering liver; C_{out}: drug concentration exiting liver.

Five representative drugs were selected for this study. Fluoxetine is a flow-limited drug [17]; tolbutamide is a capacity-limited, binding-insensitive drug [18]; and diazepam, diclofenac, and rosuvastatin are capacity-limited, binding-sensitive drugs [19–22]. First, an in silico multinomial logistic regression analysis was conducted to predict the most suitable CL_H model for binding-sensitive drugs. The "percent better prediction" (%BP) value was then used to indicate the extent to which a particular CL_H model was favored. Subsequently, an IPRL experiment was performed for each drug at different protein concentrations to measure actual CL_H, and the resulting data were subjected to statistical analysis to determine which model was more appropriate, thereby elucidating the influence of proteins on hepatic drug metabolism. These experimental findings are intended to validate the feasibility of using an in silico model selection approach for IVIVE of drugs with diverse physicochemical and pharmacokinetic properties. This method reduces the time required to identify an appropriate CL_H model and provides valuable guidance for clinical dose adjustment. Compared with our previous works that primarily focused on theoretical modeling [3,6], the current study extends the methodology by validating the logistic regression-based model selection across multiple drug classes. This integration of in silico prediction with ex situ IPRL results not only reinforces the mechanistic basis but also broadens the model applicability under varied physiological conditions.

2. Results

2.1. Logistic Regression Modeling

Based on logistic regression analysis for selecting hepatic models, the category with the highest probability, reflected by the BP%, was identified as the optimal hepatic model

(W, M, or S). None of the drugs tested exhibited the highest probability in category S. As presented in Table 1, the WSM exhibited significantly higher BP% values than the MWSM for diazepam and diclofenac (92.92% vs. 0.04% and 55.26% vs. 13.92%, respectively), indicating the superior predictive performance of the WSM for these compounds. In contrast, MWSM outperformed WSM in terms of the BP% for rosuvastatin (48.59% vs. 19.95), demonstrating MWSM's greater suitability for this drug. The other two test drugs, fluoxetine and tolbutamide, were not evaluated by logistic regression analysis. This is because fluoxetine, classified as a flow-limited drug, has metabolic characteristics inherently captured by WSM. Conversely, tolbutamide, which is categorized as a capacity-limited binding-insensitive drug, exhibited comparable predictive performance with both WSM and MWSM. In other words, both models predicted tolbutamide metabolism with similar accuracy. These results are consistent with observations from the IPRL, which are detailed in the following section.

Table 1. Multinomial logistic regression for the percent better prediction of the application of different drugs based on the well-stirred and modified well-stirred models.

Drug	Percent Better Prediction (BP%)		
	W	**S**	**M**
Diazepam	92.92	7.04	0.04
Diclofenac	55.26	30.82	13.92
Rosuvastatin	19.95	31.46	48.59

S: Similar predictive power of the two models; M: modified well-stirred model; W: well-stirred model.

2.2. Equilibrium Dialysis

The fraction unbound (f_u) of each assessed drug at various HSA concentrations was determined by RED. For diclofenac, the f_u values at 0%, 0.0025%, 0.01%, 0.025%, 0.1%, and 2% albumin were 1.000, 0.931, 0.872, 0.576, 0.164, and 0.006, respectively (Figure 2B), with the most pronounced changes occurring between 0.01% and 0.025%. Similarly, the f_u values of rosuvastatin were 0.99, 0.90, 0.77, 0.65, 0.51, 0.42, and 0.29 (Figure 2C); those of fluoxetine were 0.99, 0.87, 0.45, 0.40, and 0.05 (Figure 2D); and those of tolbutamide were 0.98, 0.60, 0.40, 0.25, and 0.13 (Figure 2E), respectively.

2.3. Drug Metabolism in IPRL

In this part of the analysis, each drug exhibited a distinct f_u at different protein concentrations. Under this condition, hepatic availability (F_H) served as a clear and practical indicator of CL_H. A higher F_H (ranging from 0 to 1) reflected a lower degree of hepatic metabolism and clearance. Based on the principles of the WSM, Equations (3) and (4) were derived by applying Equations (1) and (2), in conjunction with the concept that CL_H equals the liver blood flow multiplied by the extraction ratio. Subsequently, data fitting was performed using these formulas. Specifically, after listing the F_H equations for each CL_H model (Equations (3) and (4)) and incorporating the liver blood flow rate from the IPRL experiment (Q_H = 15 mL/min), the data points obtained from the IPRL were fitted, as shown in Figure 3, to yield the optimal intrinsic clearance (CL_{int}) for each model.

$$F_H = \frac{Q_H}{CL_{int,WSM} \cdot f_u + Q_H} \tag{3}$$

$$F_H = 1 - \frac{CL_{int,\ MWSM}}{Q_H} \cdot f_u \tag{4}$$

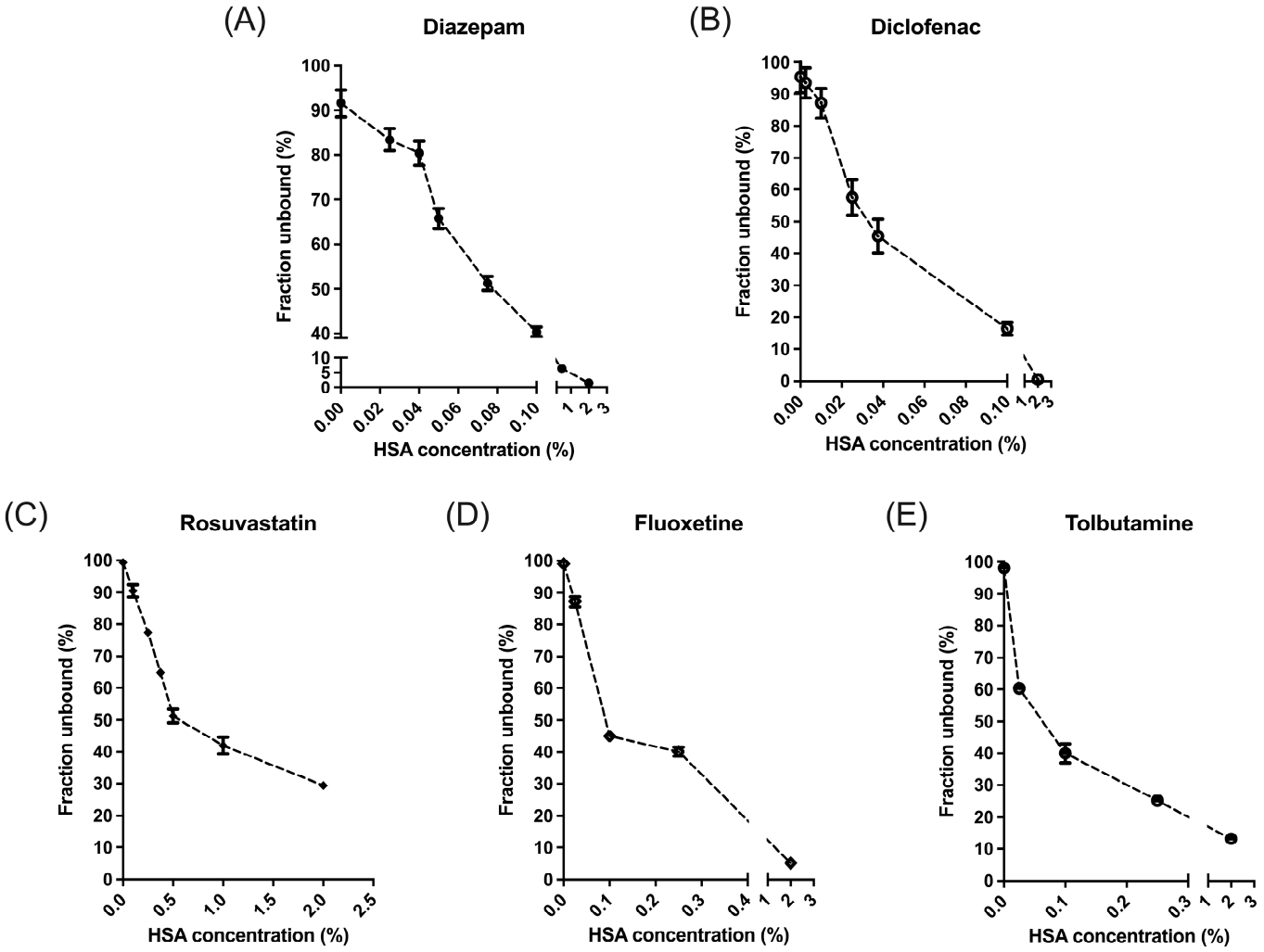


Figure 2. Different protein concentrations correspond to specific fraction unbound values using the rapid equilibrium dialysis method. (**A**) Data obtained from Hsu et al., 2021 [6]. (**B**–**E**) Data obtained in this study. The parameter f_u was the most sensitive to changes in HSA concentration. HSA: human serum albumin; f_u: fraction of unbound drug in blood.

Table 2 summarizes how the F_H for the five drugs varied at different protein (HSA) concentrations in the IPRL experiments. In addition to the WSM and MWSM discussed previously, commonly used PTM and DM were included for comparison. By substituting the f_u values from Figure 2 in place of the HSA concentrations reported in Table 2, it becomes more intuitive to determine which model more accurately characterizes the CL_H behavior of each drug, as illustrated in Figure 3. The details follow those described in our previous report [6].

As shown in Table 2, higher protein concentrations led to an increased F_H, reflecting a decrease in the fraction of drug cleared by the liver. This outcome aligns with the logic that only the free drug is metabolized. Figure 3 further illustrates that when the f_u of diazepam and diclofenac (Figure 3A,B) approaches 1, the overall F_H trends shift from closely resembling the WSM (blue line in Figure 3) to more closely matching the MWSM (brown line in Figure 3). Rosuvastatin (Figure 3C) consistently followed the MWSM pattern, highlighting the ability of MWSM to address the limitations of WSM for particular drugs. Fluoxetine (Figure 3D) appeared to display F_H profiles in which WSM was still the best model for effective capture. Based on the obtained data, fluoxetine was considered to follow the WSM pattern, consistent with the expectation that flow-limited drugs would

still be best described by the WSM for CL_H calculations [8]. Tolbutamide (Figure 3E), which was relatively insensitive to changes in protein concentration, showed similar fits under all four models, aligning well with the IPRL experimental results shown in Table 2. Thus, each model demonstrated an equivalent capacity to describe the hepatic metabolic profile.

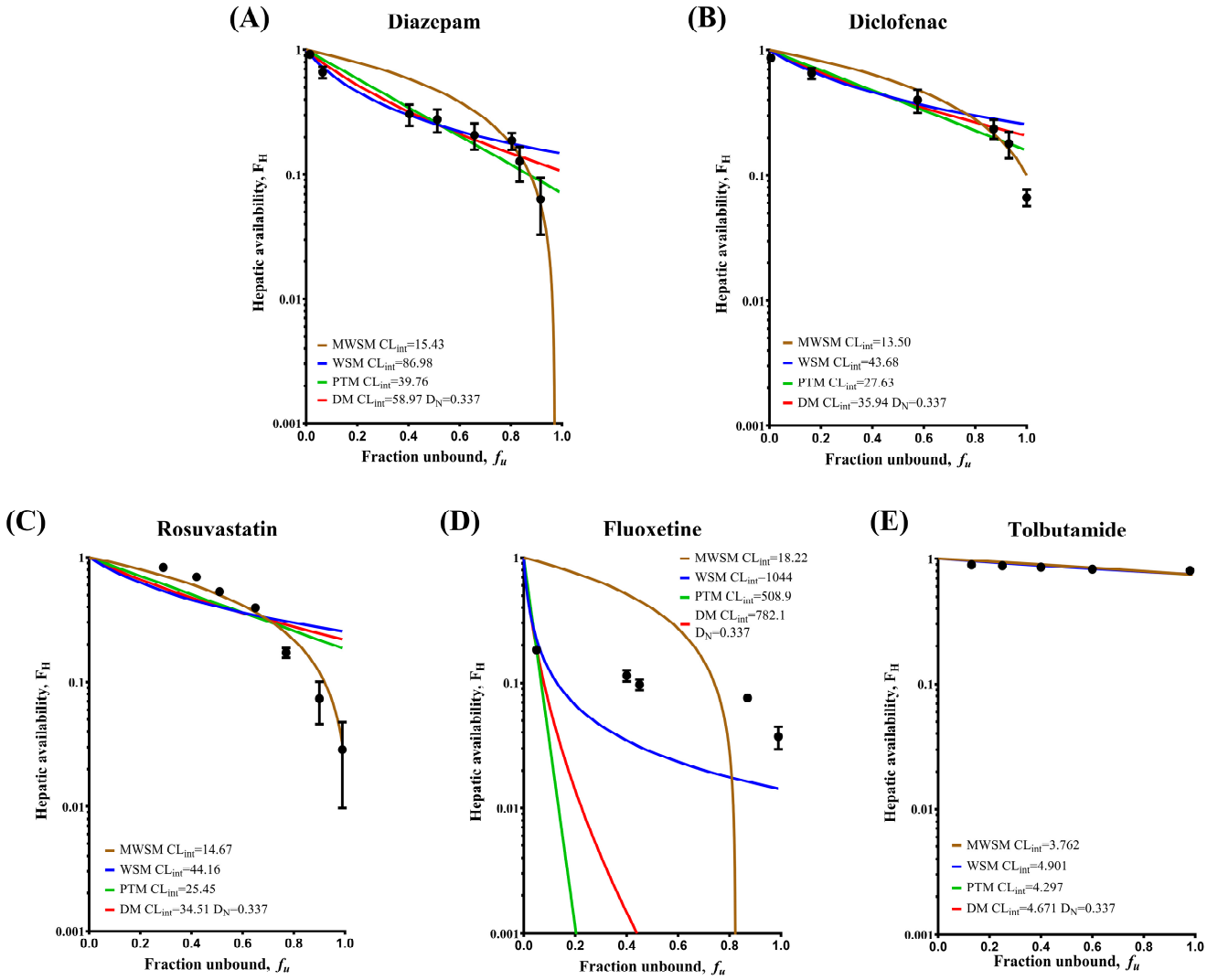


Figure 3. Differences in the hepatic availability (F_H) of different drugs at specific unbound fractions. According to an average value of f_u at the cutoff point, the simulated curves indicated in different colors were obtained using MWSM (brown), WSM (blue), PTM (green), and DM (red) models. (**A**) Data were obtained from a previous study [6]. The transformation point of diazepam is set at f_u = 0.804. MWSM is simulated using the f_u range between 0.804 and 0.916. WSM, PTM, and DM are simulated using the f_u range between 0.015 and 0.804. (**B**) The transformation point of diclofenac is set between f_u = 0.576 and 0.872. MWSM is simulated using the f_u range between 0.872 and 0.954. WSM, PTM, and DM are simulated using the f_u range between 0.006 and 0.576. (**C**–**E**) There are no transformation points for any of the assessed drugs. For each drug, all models were simulated using the entire f_u range. All points in the figure represent average IPRL values for specific protein binding with a different cutoff point. IPRL: isolated perfused rat liver; HSA: human serum albumin; f_u: fraction of unbound drug in blood; CL_{int}: intrinsic clearance; WSM: well-stirred model; MWSM: modified well-stirred model; PTM: parallel-tube model; DM: dispersion model.

Table 2. Relevant hepatic bioavailability (mean ± SD) of assessed drugs at different albumin concentrations (n number shown in parentheses).

Drug \ Concentration Sequences	1	2	3	4	5	6	7	8
Diazepam [a]	0.063 ± 0.031 (15)	0.127 ± 0.040 (15)	0.188 ± 0.029 (9)	0.208 ± 0.050 (15)	0.277 ± 0.058 (9)	0.305 ± 0.059 (15)	0.664 ± 0.070 (6)	0.920 ± 0.040 (6)
Diclofenac [b]	0.067 ± 0.010 (6)	0.180 ± 0.044 (5)	0.237 ± 0.041 (6)	0.400 ± 0.084 (6)	0.654 ± 0.064 (6)	0.869 ± 0.039 (4)	-	-
Rosuvastatin [c]	0.029 ± 0.019 (12)	0.073 ± 0.027 (6)	0.172 ± 0.015 (6)	0.395 ± 0.015 (6)	0.533 ± 0.037 (6)	0.700 ± 0.032 (6)	0.833 ± 0.039 (4)	-
Fluoxetine [d]	0.037 ± 0.008 (7)	0.076 ± 0.005 (7)	0.097 ± 0.010 (7)	0.114 ± 0.011 (7)	0.183 ± 0.010 (6)	-	-	-
Tolbutamide [d]	0.808 ± 0.030 (6)	0.828 ± 0.025 (6)	0.858 ± 0.015 (6)	0.880 ± 0.014 (6)	0.895 ± 0.014 (6)	-	-	-

The diazepam data were obtained from Hsu et al., 2021 [6]. The other data were generated in this study. The human serum albumin concentration sequence of each drug: [a] Diazepam sequence: 0%, 0.025%, 0.04%, 0.05%, 0.075%, 0.1%, 0.5%, and 2%. [b] Diclofenac sequence: 0%, 0.0025%, 0.01%, 0.025%, 0.1%, and 2%. [c] Rosuvastatin sequence: 0%, 0.1%, 0.25%, 0.375%, 0.5%, 1%, and 2%. [d] Fluoxetine and tolbutamide sequences: 0%, 0.025%, 0.1%, 0.25%, and 2%.

Different albumin concentration sequences were designed for each drug because the curve could be split into two intervals corresponding to the well-stirred model and the modified well-stirred model. This approach allowed for a more precise observation of the specific model by switching ranges for each drug.

2.4. Fitting the Model-Simulated Curves

By calculating the sum of the squares between the predicted and observed F_H values shown in Figure 3, it was possible to quantitatively determine which CL_H model best suited each drug (Table 3). Diazepam and diclofenac exhibited clear preferences for MWSM and WSM, respectively, at various HSA concentrations. Rosuvastatin consistently aligned with the MWSM predictions throughout the experiment. As anticipated, fluoxetine aligned more closely with the WSM, as evidenced by its lowest sum of squares value among all the tested models, indicating that the WSM remained the most suitable. Tolbutamide, the representative binding-insensitive, capacity-limited drug, showed sum of squares values below 0.1 for all models. This outcome indicated that all models could accurately predict the CL_H of tolbutamide, which is associated with a poor degree of liver metabolism.

Table 3. Degree of fit of different models and HSA subgroups based on the sum of squares.

Drug	Interval of HSA Concentration (%)	Optimal Model	Modified WSM	WSM	PTM	DM
Diazepam	0–0.04	MWSM	0.0481	0.1123	0.0894	0.1003
	0.04–2	WSM	1.5150	0.1818	0.4375	0.2781
Diclofenac	0–0.01	MWSM	0.0278	0.0885	0.0702	0.0792
	0.025–2	WSM	0.2923	0.1194	0.1790	0.1400
Rosuvastatin	0–2	MWSM	0.2132	1.8440	1.0670	1.4550
Fluoxetine	0–2	WSM	5.9630	0.1154	0.2096	0.2062
Tolbutamide	0–2	WSM	0.0923	0.0672	0.0790	0.0715

Data for diazepam were obtained from a study by Hsu et al., 2021 [6]. The other data were generated in this study. WSM: well-stirred model; PTM: parallel-tube model; DM: dispersion model; HSA: human serum albumin.

3. Discussion

As shown in Figure 3 and Table 3, diazepam and diclofenac, both binding-sensitive capacity-limited drugs, exhibited a marked shift in model predictability as the protein concentration varied. This phenomenon can be explained by Equations (3) and (4), as shown

in Figure 4. The underlying concept for Figure 4 is rooted in the free-drug hypothesis: If f_u is zero, no drug is available for metabolism. Thus, both the WSM and MWSM curves begin from the point $F_H, f_u = (1, 0)$.

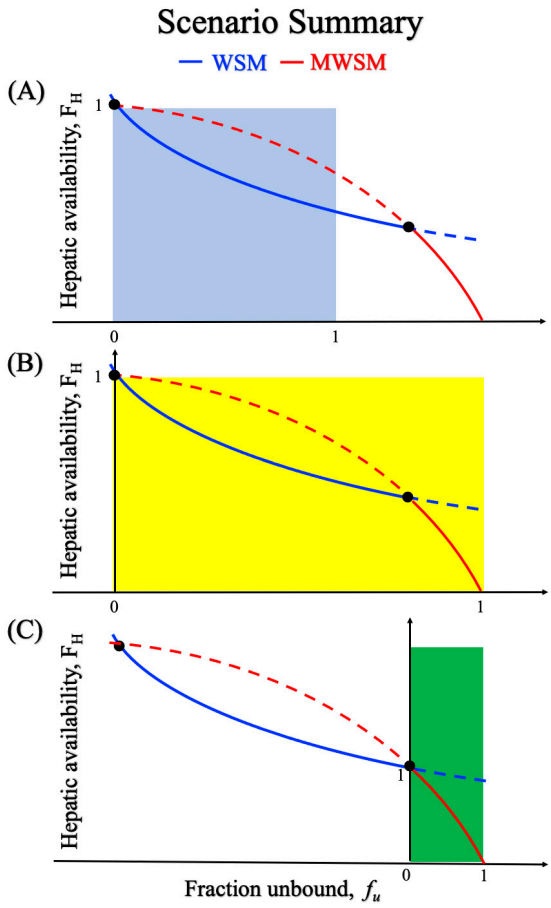


Figure 4. Four scenarios related to the classification of capacity-limited, binding-sensitive drugs. (**A**) The metabolism of the drugs in this scenario will always follow WSM. (**B**) When f_u varies between 0 and 1, two intersection points will appear, indicating that as f_u increases, the drug metabolism pattern will shift from WSM to MWSM. (**C**) In this scenario, drug metabolism consistently follows MWSM. Brown line: modified well-stirred model (MWSM); blue line: well-stirred model (WSM); black intersection point: the transition point of the metabolism model.

To elucidate this phenomenon, Figure 4 is divided into three scenarios. As shown in Figure 4A, the drug was metabolized efficiently by the liver, leading the F_H to align with the WSM trend under all f_u values. The flow-limited drug, fluoxetine, served as an example. Figure 4B illustrates the situation for diazepam and diclofenac, where increasing f_u prompts a transition from WSM to MWSM. Figure 4C shows that rosuvastatin consistently followed the MWSM trend, indicating the necessity of using the MWSM in liver metabolism research. For a capacity-limited, binding-sensitive drug, determining whether its behavior aligns more closely with scenario B or C requires a multifaceted approach, including in silico methods, to enhance the accuracy of IVIVE in predicting hepatic metabolic profiles.

In contrast to the aforementioned drugs, fluoxetine is considered to be representative of the flow-limited group of drugs, all of which are highly metabolized regardless of their protein-binding levels. Our IPRL results revealed a sharp decline in bound fluoxetine at high albumin concentration intervals, and the MWSM could not predict such rapid reductions in F_H at such high albumin concentrations (Figure 3D). Therefore, these drugs can only be described using WSM to depict their metabolic profiles.

Drugs in the binding-insensitive group undergo minimal metabolism in the liver (low extraction ratio, ER); in this regard, we selected tolbutamide to verify the in silico-based model selection method. However, the poor metabolism of the drugs in this group resulted in only minimal metabolic differences among the different models, with all models showing similar predictive abilities.

Before exploring the effects of protein binding on CL_H, it is instructive to systematically review the underlying assumptions of currently used CL_H models to clarify some often-overlooked conceptual details. The apparent differences among these models, including WSM, PTM, DM, and MWSM, stem from the conceptualization of drug distribution within the liver. This distinction manifests as different "driving force concentrations" (C_{DF}) in the derivation of the equations of each model. Specifically, CL_H is defined as the ratio of the elimination rate of a drug to its concentration during metabolism (C_x), as shown in Equation (5):

$$CL = \frac{dx/dt}{C_x} = \frac{v}{C_x} \tag{5}$$

Under liver conditions, two primary assumptions are made: (1) at steady state, the instantaneous change in the elimination rate of a drug is zero, and (2) the proportion of biliary excretion is negligible. Consequently, changes in drug concentration are predominantly governed by liver metabolism. Under these conditions, the numerator in Equation (5) can be expressed as Equation (6):

$$v = \frac{dx}{dt} = Q \cdot C_{in} - Q \cdot C_{out} \tag{6}$$

From a microscopic perspective, drug metabolism in the liver proceeds when free drug molecules bind to liver enzymes and undergo metabolic reactions (as illustrated in Equations (7) and (8)):

$$CL_{int} = \frac{\frac{dx}{dt}}{C_x \cdot f_u} = \frac{Q \cdot C_{in} - Q \cdot C_{out}}{C_x \cdot f_u} \tag{7}$$

$$CL_{int} \cdot f_u \cdot C_x = Q \cdot C_{in} - Q \cdot C_{out} \tag{8}$$

In standard CL_H derivations, concentration C_x is assumed to equal C_{out} [7]. Rearranging the terms provides the expression for C_{in} (Equation (9)). Substituting this into Equation (10) yields the classic form of the WSM (Equation (1)).

$$C_{in} = \frac{C_{out} \cdot (Q + CL_{int} \cdot f_u)}{Q} \tag{9}$$

$$CL_H = Q \cdot ER = Q \cdot \frac{C_{in} - C_{out}}{C_{in}} \tag{10}$$

In the other CL_H models, C_x in Equation (8) is substituted with what each model deems to be the "true" C_{DF} during hepatic drug metabolism. Nevertheless, these three critical points warrant further examination.

1. When protein binding occurs, does the variation in the concentration of the free drug influence the accuracy of model predictions, and if so, in what way?
2. WSM designates C_{out} as the C_{DF}. What are the reasons behind this choice and what mechanisms could validate this assumption?
3. While Equation (10) has long been regarded as practical and intuitive from a macroscopic perspective, questions remain regarding its universal applicability.

Previous experimental findings for diazepam and diclofenac indicate that when f_u approaches 1, the optimal predictive model shifts from WSM to MWSM. In its derivation,

the only difference between the MWSM and WSM is that the former designates C_{in}, rather than C_{out}, as the C_{DF}. This observation suggests that when a drug exists predominantly in its free form, the C_{DF} more closely approximates C_{in}. In reality, a drug experiences several physicochemical processes, including diffusion, partitioning, and transmembrane transport, before encountering liver enzymes, and its concentration upon reaching these enzymes is unlikely to be exactly C_{in}. This scenario becomes especially relevant when protein binding is considered, as a certain fraction of the drug is initially unable to undergo metabolism (assuming that protein-facilitated uptake or dissociation is minimal). Consequently, for binding-sensitive drugs, the C_{DF} is effectively reduced by protein binding and is therefore closer to C_{out} (as assumed by the WSM). However, once f_u increases sufficiently, the greater availability of the free drug increases the C_{DF} closer to C_{in} (as assumed by the MWSM). Hence, whenever the C_{DF} is altered by the complexity of the metabolic environment, the choice of the CL_H model depends on whether this concentration is closer to C_{in} or C_{out}. Much of our investigation of CL_H models focused on these distinctions. IPRL experiments with binding-sensitive, capacity-limited drugs have provided empirical evidence confirming that these considerations have practical relevance beyond mere theoretical constructs.

Flow-limited drugs are also susceptible to protein-binding effects. Why do they not exhibit model shifts when f_u changes? This situation arises because drugs with high ER are considered "flow-limited," implying that for the specific drug, the metabolic capacity of the liver is so great that any incoming drug is immediately metabolized, leaving liver blood flow as the only limiting factor. Interestingly, this description inherently aligns with the fundamental assumption of the WSM, namely that once the drug enters the liver, it is instantaneously distributed and metabolized throughout the organ. In reality, whether a drug is readily metabolized in the liver depends on two factors: (1) how easily free drug molecules travel from the bloodstream to the metabolic enzymes and (2) the intrinsic capacity of those enzymes to metabolize the drug. A compound that perfectly conforms to the WSM predictions would exhibit both a very high distribution potential (related to its physicochemical properties) and an especially high enzymatic capacity (pharmacokinetic attribute). However, not every high-ER drug satisfies these two criteria. Whenever either condition is not met, WSM-based predictions can become inaccurate and potentially deviate from the observed values by more than twofold [23]. This consideration helps clarify why fluoxetine, although appearing to follow the WSM to a great extent, still does not perfectly match the WSM predictions [17,24].

Although Equation (10), adapted from chemical engineering principles, was introduced early in the development of the CL_H theory and underlies most current CL_H models, related discussions remain active in this area. For instance, Benet et al. re-examined Equation (10) and its assumptions from the perspective of the C_{DF} [25] and further indicated that Equation (8) is flow independent, whereas Equation (10) is flow dependent, making it evident that the two are not connectable [26]. While the ER in Equation (10) can represent, on a macro scale, the proportion of drugs metabolized by the liver and is thus linked to the concept of CL_H, it cannot be equated directly to Equation (8), which describes the microscopic behavior of drug molecules during metabolism. This misalignment in descriptive focus can introduce complications in the complex environment of the liver and is a possible reason for the widespread underestimation of CL_H in IVIVE [27]. Currently, only drugs with minimal hepatic metabolism, such as tolbutamide, appear to be unaffected by this discrepancy, leading to consistent metabolic profiles across various models.

In summary, selecting the most suitable CL_H model begins with a three-phase classification of drugs. As shown in Figure 1, for capacity-limited, binding-sensitive drugs, multinomial logistic regression is crucial for determining the appropriate model; however, variations in f_u for such drugs may result in a shift in the predictive model between WSM

and MWSM. In contrast, WSM consistently provides the most accurate predictions for flow-limited drugs, whereas both WSM and MWSM exhibit comparable predictive accuracies for capacity-limited, binding-insensitive drugs. In addition, to the best of our knowledge, few studies have addressed the impact of hypoalbuminemia on CL_H model selection. Our findings emphasize that the prediction models of CL_H should not remain fixed but should instead be adjusted in response to changes in physiological albumin concentrations. Under hypoalbuminemic conditions, certain clinical drugs may require distinct CL_H models to determine the proper dose. Since hypoalbuminemia is frequently observed in clinical scenarios such as chronic liver disease, malnutrition, and severe inflammation [28–32], accurate model selection under abnormal albumin levels is critical to avoid dosing errors and ensure therapeutic efficacy.

4. Materials and Methods

4.1. Logistic Regression Modeling for Hepatic Model Selection

In accordance with a previous study, we utilized multinomial logistic regression to predict the optimal hepatic model, either WSM or MWSM, for the selected compounds [3]. A formula (Equation (11)) was developed from the data on 223 compounds, incorporating 16 detailed physicochemical and pharmacokinetic parameters. The dependent variable representing the most suitable hepatic model was classified into three categories: W (WSM provides better predictions), M (MWSM provides better predictions), and S (both models yield equally accurate predictions). The probability of each outcome was determined by using a multinomial logistic regression formula (Equation (11)). The sum of all probabilities was 1.

$$P(Y = k \mid X) = \frac{\exp\left(\beta_{k0} + \beta_{k1}X_1 + \beta_{k2}X_2 + \ldots + \beta_{kp}X_p\right)}{1 + \sum_{j=1}^{K-1} exp\left(\beta_{j0} + \beta_{j1}X_1 + \beta_{j2}X_2 + \ldots + \beta_{jp}X_p\right)} \quad (11)$$

where P(Y = k | X) represents the probability of a compound being classified into a specific category. X_1, X_2, … X_p are independent variables, including physicochemical and pharmacokinetic properties such as intrinsic clearance (CL_{int}), protein-binding characteristics, and distribution volume (V_{ss}). β_{kj} denotes the regression coefficients for category k and variable X_j. k is the total number of categories (k = 3, corresponding to W, M, and S).

The probabilities for model classification were derived from compound-specific physicochemical and pharmacokinetic properties, which are critical for understanding drug–hepatic metabolic interactions. Our previous study used 16 independent variables for analysis based on their theoretical relevance to drug metabolic behavior in the liver. These variables included intrinsic clearance, protein-binding characteristics (e.g., unbound fraction), and distribution volume (Table 4).

Diazepam, diclofenac, and rosuvastatin, which are classified as capacity-limited (binding-sensitive) drugs, were selected to estimate their probabilities for hepatic metabolism model classification. These probabilities were expressed as BP%. For each compound, multinomial logistic regression was used to calculate the category probability, with the highest category probability designated as the optimal hepatic model (W, M, or S). Additionally, fluoxetine and tolbutamide, which are categorized as flow-limited and capacity-limited (binding-insensitive) drugs, respectively, were included in this study. We aimed to demonstrate that these two drugs could be distinctly classified into hepatic metabolism models based on their intrinsic characteristics, without the need for multinomial logistic regression analysis. All relevant statistical analyses related to multinomial logistic regression were performed using SPSS Statistics 28 (IBM Corporation, Armonk, NY, USA). Statistical significance was determined using two-tailed p-values, with values of less than 0.05 considered indicative of a significant effect.

Table 4. Multinomial logistic regression datasets.

Drug	MW [a]	AlogP [a]	PSA [a]	Rotatable Bonds [a]	HBA [a]	HBD [a]	Aromatic Rings [a]	Heavy Atoms [a]	V_{ss} [b]	MRT [b]	$logCL_{int,u,in\text{-}vivo}$ (pred)		fu_p	Class [a]	OATP [c]	P-gp [c]
											hep	mic				
Diazepam	285	3.15	32.67	1	3	0	2	20	1.00	44.00	0.93	0.95	0.021	N	Without	With
Diclofenac	296	4.36	49.33	4	3	2	2	19	0.22	1.00	2.24	2.17	0.004	A	Without	Without
Rosuvastatin	482	2.4	140.9	10	9	3	2	33	1.70	2.60	1.30	NF	0.129	A	With	Without

NF: not found; S: group of compounds with similarly accurate prediction in both hepatic models; M: group of compounds with better prediction using the modified well-stirred model; W: group of compounds with better prediction using the well-stirred model; MW: molecular weight; AlogP: partition coefficient; PSA: polar surface area; HBA: hydrogen-bond acceptor; HBD: hydrogen-bond donor; V_{ss}: volume of distribution at steady state; $logCL_{int,u,in\text{-}vivo}$ (pred): logarithm of predicted in vivo unbound intrinsic clearance; hep: hepatocytes; mic: microsome; fu_p: fraction unbound in plasma; A: acidic; N: neutral; OATP: organic anion-transporting polypeptide; P-gp: p-glycoprotein. [a] Data obtained from the EMBL-EBI database. R_b was set to 1 for basic or neutral compounds and 0.55 for acidic compounds when the experimental value was unavailable in the original studies [33,34]. [b] Data obtained from Lombarbo et al. [35] and DrugBank. [c] Data obtained from El-Kattan et al. [36] and DrugBank.

4.2. Chemicals

Diclofenac, rosuvastatin, fluoxetine, tolbutamide, atorvastatin, naproxen, and diazepam were purchased from Thermo Fisher Scientific (Bellefonte, PA, USA), Pfizer (New York City, NY, USA), Acros Organics (Geel, Belgium), Sigma-Aldrich (St. Louis, MO, USA), CombiBlocks (San Diego, CA, USA), and Cerilliant (Round Rock, TX, USA). The perfusion buffer used for the IPRL experiments consisted of taurocholate, sodium bicarbonate, and commercial Krebs–Ringer powder obtained from Acros Organics (Merck, Taipei, Taiwan) and Sigma-Aldrich. Fatty acid-free human serum albumin (HSA) was obtained from SeraCare (Milford, MA, USA).

4.3. Rapid Equilibrium Dialysis

The rapid equilibrium dialysis (RED) apparatus and test inserts were purchased from Thermo Fisher Scientific (Rockford, IL, USA). The unbound fraction of each assessed drug was determined using RED. Briefly, a drug was diluted to 1 μg/mL in Krebs buffer containing different concentrations of HSA. Five hundred microliters of the assessed drug and each of the different HSA concentrations were added to the sample chamber of an insert and 750 μL of blank buffer was added to the adjacent chamber. The loaded inserts were then assembled on a Teflon-based plate. The plate was then sealed with a self-adhesive lid and agitated at 20 rpm and 37 ± 1 °C using an oscillating shaker (Genepure Rocking Shaker, OSR205-01) for 8 h.

4.4. Surgery and Liver Perfusion

Male Sprague–Dawley rats (350–450 g; BioLASCO Co., Ltd., Taipei, Taiwan) were housed at the Laboratory Animal Center of the National Defense Medical Center and provided free access to water and food with a 12 h light/dark cycle. All animal experiments were approved by the Institutional Animal Care and Use Committee of the National Defense Medical Center (IACUC-20-164, Taipei, Taiwan) on 7 May 2020. Anesthesia, surgical procedures, and perfusion were performed as previously described [6]. The surgery and liver perfusion were executed at the National Defense Medical Center from 2020 to 2024. Perfusates containing the assessed drugs and different concentrations of HSA were freshly prepared and maintained at 4 °C after mixing. All cycles lasted 20 min. For each cycle, samples were collected at 16, 17, 18, 19, and 20 min after incubation. At the end of each IPRL experiment, the rat liver was perfused with HSA-free Krebs buffer as a quality control measure to confirm enzymatic activity. In different perfusion cycles, the livers were perfused with buffer containing HSA in a sequence from low to high concentrations to minimize cross-contamination and other confounding factors. Bile elimination can be disregarded because it accounts for only 0.2% of total metabolism [7].

4.5. Sample Preparation and Analysis

A perfusate sample (400 μL) containing diclofenac was combined with 80 μL (1 μg/mL) of naproxen (internal standard, IS), 150 μL of 1% formic acid, and 2 mL of extraction solvent (ethyl acetate: *n*-hexane = 2:3). The mixture was vortexed for 5 min, and the resulting upper organic phase was collected, dried, reconstituted in 80% methanol, and used to inject rats for experiments. In addition, 100 μL of perfusate samples containing rosuvastatin, fluoxetine, and tolbutamide were combined with 20 μL (1 μg/mL) of IS (atorvastatin, diazepam, and diazepam) and 10 μL of 0.1% formic acid. The mixture was extracted using an Oasis HLB 1cc extraction cartridge.

For the separation of diclofenac, we used Thermos BDS Hypersil C18 columns (4.6 × 100 mm, 5 mm; Thermo Fisher Scientific, Waltham, MA, USA); for the separation of rosuvastatin, fluoxetine, and tolbutamide, we used Waters Symmetry C18 columns (2.1 × 100 mm, 1.7 μm; Waters Corporation, Milford, MA, USA).

The column separation of diclofenac, rosuvastatin, fluoxetine, and tolbutamide was achieved using isocratic elution with different mobile phase compositions tailored to each compound. Diclofenac was separated using a mobile phase of 2 mM ammonium acetate and 0.1% formic acid in water mixed with 2 mM ammonium acetate and 0.1% formic acid in methanol in a 1:9 ratio. For rosuvastatin, the mobile phase consisted of 0.1% formic acid in water and 0.1% formic acid in a mixture of 90% acetonitrile and 10% methanol in a 1:3 ratio. Fluoxetine was analyzed using a mobile phase of 0.1% formic acid in water and 0.1% formic acid in acetonitrile in a 3:7 ratio. The separation of tolbutamide was conducted using 0.1% formic acid in water and 0.1% formic acid in methanol in a 1:4 ratio.

For the analysis of diclofenac (296.1/250.0), naproxen (231.3/185.0), rosuvastatin (482.0/258.0), atorvastatin (560.3/441.1), fluoxetine (310.2/44.2), and diazepam (285.1/154.0), the samples were analyzed by the ionization interface of an Applied Biosystems-Sciex API 3000 series triple-quadrupole mass spectrometer (Foster City, CA, USA) with an Agilent Technologies 1200 series high-performance liquid chromatograph (Böeblingen, Germany). For that of tolbutamide (271.1/91.1) and diazepam (285.1/193.0), the samples were measured by a Shimadzu Nexera LC-40B X3 ultrahigh-performance liquid chromatograph (Böblingen, Germany) with a Biosystems-Sciex API 4000 series triple-quadrupole mass spectrometer (Foster City, CA, USA). The extraction recovery, calibration curves and retention time of each compound are shown in Table S1, Figures S1 and S2, respectively. All available experimental data were included in the analysis. The formula and experimental data were processed by Prism software v10.4.1 (GraphPad Software, Inc) to generate figures and calculate the degree of fit of different models.

5. Conclusions

This study demonstrates the importance of appropriate model selection for accurately predicting CL_H using an IVIVE method. By conducting experiments using an IPRL system, we validated the utility of the in silico-based model selection method for distinguishing between the WSM and MWSM models for predicting CL_H across diverse drug categories. These findings underscore the importance of model selection in optimizing CL_H predictions and emphasize the value of tailoring CL_H models to the unique characteristics of each drug, with significant implications for dosing adjustments and clinical decision-making, particularly in patients with varying albumin levels.

Supplementary Materials: The following supporting information can be downloaded at: https://www.mdpi.com/article/10.3390/ph18070991/s1, Table S1: Extraction recovery (%) of diazepam, diclofenac, rosuvastatin, fluoxetine, and tolbutamide determined by LC–MS/MS analyses (n = 3); Figure S1: Calibration curves of the tested drugs (A–E) used in IPRL analysis; Figure S2: Liquid chromatography mass spectrometry of diazepam, diclofenac, rosuvastatin, fluoxetine, tolbutamide, and internal standard (IS) in Krebs buffer.

Author Contributions: R.-J.L.: conceptualization, methodology, formal analysis, data curation, writing—original draft, writing—review and editing, visualization, project administration, funding acquisition. S.-H.H.: conceptualization, methodology, validation, formal analysis, investigation, data curation, writing—original draft, writing—review and editing, visualization. H.-T.C.: conceptualization, writing—review and editing. W.-H.C.: writing—review and editing. H.-Y.F.: writing—review and editing, visualization. H.-Y.C.: formal analysis, investigation, data curation, writing—review and editing. H.-J.W.: conceptualization, methodology, validation, resources, writing—review and editing, visualization, supervision, project administration, funding acquisition. S.-L.T.: validation, resources, writing—review and editing, supervision, project administration. All authors have read and agreed to the published version of the manuscript.

Funding: This study was financially supported by the National Science and Technology Council, Taipei, Taiwan [NSCT 113-2320-B-016-003-MY2]; the Tri-Service General Hospital Keelung Branch, Keelung, Taiwan [TSGH-KL_E_114007]; and the Ministry of National Defense, Taiwan [MND-MAB-D-113119].

Institutional Review Board Statement: The animal study protocol was approved by the Institutional Animal Care and Use Committee of the National Defense Medical Center (protocol code IACUC-20-164, approved on 7 May 2020).

Data Availability Statement: The authors declare that all data supporting the findings of this study are contained within the article or Supplementary Materials.

Acknowledgments: We would like to thank Nathan Shyu (University of California, Irvine) for assistance in enhancing the quality of this manuscript. Additionally, we sincerely appreciate Li-Ting Kao for her valuable assistance in the statistical analysis for this study.

Conflicts of Interest: The authors declare no conflicts of interest.

Abbreviations

The following abbreviations are used in this manuscript:

C_{DF}	Driving force concentrations
C_{DM}	Representative drug concentration in DM
C_H	Total drug concentration in liver
C_{in}	Drug concentration entering liver
CL_H	Hepatic clearance
CL_{int}	Intrinsic clearance
C_{MWSM}	Representative drug concentration in MWSM
C_{out}	Drug concentration exiting liver
C_{PTM}	Logarithmic mean drug concentration in PTM
C_{WSM}	Representative drug concentration in WSM
DM	Dispersion model
ER	Extraction ratio
F_H	Hepatic availability
f_u	Intravascular fraction of unbound drug
$f_{u,E}$	Extravascular fraction of unbound drug
HSA	Human serum albumin
IPRL	Isolated perfused rat liver
IVIVE	In vitro-to-in vivo extrapolation
MWSM	Modified well-stirred model
PTM	Parallel-tube model
Q_H	Hepatic blood flow
WSM	Well-stirred model

References

1. Rowland, M. Influence of Route of Administration on Drug Availability. *J. Pharm. Sci.* **1972**, *61*, 70–74. [CrossRef] [PubMed]
2. Benet, L.Z.; Sodhi, J.K. Investigating the Theoretical Basis for In Vitro–In Vivo Extrapolation (IVIVE) in Predicting Drug Metabolic Clearance and Proposing Future Experimental Pathways. *AAPS J.* **2020**, *22*, 120. [CrossRef] [PubMed]
3. Chang, T.-Y.; Wang, H.-J.; Hsu, S.-H.; Chang, M.-L.; Kao, L.-T.; Pao, L.-H. Evidence of the Need for Modified Well-Stirred Model in Vitro to in Vivo Extrapolation. *Eur. J. Pharm. Sci.* **2022**, *177*, 106268. [CrossRef]
4. Diaz-Garcia, J.M.; Evans, A.M.; Rowland, M. Application of the Axial Dispersion Model of Hepatic Drug Elimination to the Kinetics of Diazepam in the Isolated Perfused Rat Liver. *J. Pharmacokinet. Biopharm.* **1992**, *20*, 171–193. [CrossRef]
5. Dong, J.; Park, M.S. Discussions on the Hepatic Well-Stirred Model: Re-Derivation from the Dispersion Model and Re-Analysis of the Lidocaine Data. *Eur. J. Pharm. Sci.* **2018**, *124*, 46–60. [CrossRef]
6. Hsu, S.-H.; Cheng, A.-C.; Chang, T.-Y.; Pao, L.-H.; Hsiong, C.-H.; Wang, H.-J. Precisely Adjusting the Hepatic Clearance of Highly Extracted Drugs Using the Modified Well-Stirred Model. *Biomed. Pharmacother.* **2021**, *141*, 111855. [CrossRef] [PubMed]
7. Pang, K.S.; Rowland, M. Hepatic Clearance of Drugs. I. Theoretical Considerations of a "Well-Stirred" Model and a "Parallel Tube" Model. Influence of Hepatic Blood Flow, Plasma and Blood Cell Binding, and the Hepatocellular Enzymatic Activity on Hepatic Drug Clearance. *J. Pharmacokinet. Biopharm.* **1977**, *5*, 625–653. [CrossRef]
8. Pang, K.S.; Rowland, M. Hepatic Clearance of Drugs. II. Experimental Evidence for Acceptance of the "Well-Stirred" Model over the "Parallel Tube" Model Using Lidocaine in the Perfused Rat Liverin Situ Preparation. *J. Pharmacokinet. Biopharm.* **1977**, *5*, 655–680. [CrossRef]
9. Roberts, M.S.; Rowland, M. A Dispersion Model of Hepatic Elimination: 3. Application to Metabolite Formation and Elimination Kinetics. *J. Pharmacokinet. Biopharm.* **1986**, *14*, 289–308. [CrossRef]
10. Rowland, M.; Pang, K.S. Commentary on "The Universally Unrecognized Assumption in Predicting Drug Clearance and Organ Extraction Ratio". *Clin. Pharmacol. Ther.* **2018**, *103*, 386–388. [CrossRef]
11. Pang, K.S.; Han, Y.R.; Noh, K.; Lee, P.I.; Rowland, M. Hepatic Clearance Concepts and Misconceptions: Why the Well-Stirred Model Is Still Used Even Though It Is Not Physiologic Reality? *Biochem. Pharmacol.* **2019**, *169*, 113596. [CrossRef]
12. Sodhi, J.K.; Wang, H.-J.; Benet, L.Z. Are There Any Experimental Perfusion Data That Preferentially Support the Dispersion and Parallel-Tube Models over the Well-Stirred Model of Organ Elimination? *Drug Metab. Dispos.* **2020**, *48*, 537–543. [CrossRef] [PubMed]
13. Wang, H.-J.; Benet, L.Z. Protein Binding and Hepatic Clearance: Re-Examining the Discrimination between Models of Hepatic Clearance with Diazepam in the Isolated Perfused Rat Liver Preparation. *Drug Metab. Dispos.* **2019**, *47*, 1397–1402. [CrossRef] [PubMed]
14. Paumgartner, G. *The Liver. Quantitative Aspects of Structure and Function: 1st International Gstaad Symposium, Organized by the Swiss Society for Gastroenterology, Gstaad, September 1972: Proceedings*; Karger Medical and Scientific Publishers: Basel, Switzerland, 1973; ISBN 978-3-318-05184-1.
15. Robert, M.S.; Rowland, M. Hepatic Eliminatilon—Dispersion Model. *J. Pharm. Sci.* **1985**, *74*, 585–587. [CrossRef]
16. Blaschke, T.F. Protein Binding and Kinetics of Drugs in Liver Diseases. *Clin. Pharmacokinet.* **1977**, *2*, 32–44. [CrossRef] [PubMed]
17. Bteich, M.; Poulin, P.; Piette, S.; Haddad, S. Impact of Extensive Plasma Protein Binding on the In Situ Hepatic Uptake and Clearance of Perampanel and Fluoxetine in Sprague Dawley Rats. *J. Pharm. Sci.* **2020**, *109*, 3190–3205. [CrossRef]
18. Schary, W.L.; Rowland, M. Protein Binding and Hepatic Clearance: Studies with Tolbutamide, a Drug of Low Intrinsic Clearance, in the Isolated Perfused Rat Liver Preparation. *J. Pharmacokinet. Biopharm.* **1983**, *11*, 225–243. [CrossRef]
19. Rowland, M.; Leitch, D.; Fleming, G.; Smith, B. Protein Binding and Hepatic Clearance: Discrimination between Models of Hepatic Clearance with Diazepam, a Drug of High Intrinsic Clearance, in the Isolated Perfused Rat Liver Preparation. *J. Pharmacokinet. Biopharm.* **1984**, *12*, 129–147. [CrossRef]
20. Hussein, Z.; Evans, A.M.; Rowland, M. Physiologic Models of Hepatic Drug Clearance: Influence of Altered Protein Binding on the Elimination of Diclofenac in the Isolated Perfused Rat Liver. *J. Pharm. Sci.* **1993**, *82*, 880–885. [CrossRef]
21. Hanke, N.; Gómez-Mantilla, J.D.; Ishiguro, N.; Stopfer, P.; Nock, V. Physiologically Based Pharmacokinetic Modeling of Rosuvastatin to Predict Transporter-Mediated Drug-Drug Interactions. *Pharm. Res.* **2021**, *38*, 1645–1661. [CrossRef]
22. Luvai, A.; Mbagaya, W.; Hall, A.S.; Barth, J.H. Rosuvastatin: A Review of the Pharmacology and Clinical Effectiveness in Cardiovascular Disease. *Clin. Med. Insights Cardiol.* **2012**, *6*, CMC.S4324. [CrossRef] [PubMed]
23. Wood, F.L.; Houston, J.B.; Hallifax, D. Clearance Prediction Methodology Needs Fundamental Improvement: Trends Common to Rat and Human Hepatocytes/Microsomes and Implications for Experimental Methodology. *Drug Metab. Dispos.* **2017**, *45*, 1178–1188. [CrossRef] [PubMed]
24. Caccia, S.; Cappi, M.; Fracasso, C.; Garattini, S. Influence of Dose and Route of Administration on the Kinetics of Fluoxetine and Its Metabolite Norfluoxetine in the Rat. *Psychopharmacology* **1990**, *100*, 509–514. [CrossRef]
25. Benet, L.; Liu, S.; Wolfe, A. The Universally Unrecognized Assumption in Predicting Drug Clearance and Organ Extraction Ratio. *Clin. Pharmacol. Ther.* **2018**, *103*, 521–525. [CrossRef]

26. Benet, L.; Sodhi, J. Can In Vitro–In Vivo Extrapolation Be Successful? Recognizing the Incorrect Clearance Assumptions. *Clin. Pharmacol. Ther.* **2021**, *111*, 1022–1035. [CrossRef]
27. Cheng, H.-C.; Chen, H.-T.; Chen, H.-Y.; Chou, N.-H.; Wang, H.-J.; Pao, L.-H.; Tang, S.-L. Advancing Hepatic Clearance Prediction across In Vitro, Ex Situ, and In Vivo Systems to Facilitate In Vitro-to-In Vivo Extrapolation. *Eur. J. Pharm. Sci.* **2025**, *212*, 107171. [CrossRef] [PubMed]
28. Banh, H.L.; Burton, M.E.; Sperling, M.R. Interpatient and Intrapatient Variability in Phenytoin Protein Binding. *Ther. Drug Monit.* **2002**, *24*, 379. [CrossRef]
29. Soeters, P.B.; Wolfe, R.R.; Shenkin, A. Hypoalbuminemia: Pathogenesis and Clinical Significance. *J. Parenter. Enter. Nutr.* **2019**, *43*, 181–193. [CrossRef]
30. Ulldemolins, M.; Roberts, J.A.; Rello, J.; Paterson, D.L.; Lipman, J. The Effects of Hypoalbuminaemia on Optimizing Antibacterial Dosing in Critically Ill Patients. *Clin. Pharmacokinet.* **2011**, *50*, 99–110. [CrossRef]
31. Bar-Or, D.; Rael, L.T.; Bar-Or, R.; Slone, D.S.; Craun, M.L. The Formation and Rapid Clearance of a Truncated Albumin Species in a Critically Ill Patient. *Clin. Chim. Acta* **2006**, *365*, 346–349. [CrossRef]
32. Zemlin, A.E.; Burgess, L.J.; Engelbrecht, A. Two Cases of Severe Hypoalbuminemia (<10 g/L). *Nutrition* **2009**, *25*, 1006–1010. [CrossRef] [PubMed]
33. Fagerholm, U. Prediction of Human Pharmacokinetics—Evaluation of Methods for Prediction of Hepatic Metabolic Clearance. *J. Pharm. Pharmacol.* **2007**, *59*, 803–828. [CrossRef] [PubMed]
34. Masimirembwa, C.M.; Bredberg, U.; Andersson, T.B. Metabolic Stability for Drug Discovery and Development. *Clin. Pharmacokinet.* **2003**, *42*, 515–528. [CrossRef] [PubMed]
35. Lombardo, F.; Berellini, G.; Obach, R.S. Trend Analysis of a Database of Intravenous Pharmacokinetic Parameters in Humans for 1352 Drug Compounds. *Drug Metab. Dispos.* **2018**, *46*, 1466–1477. [CrossRef]
36. El-Kattan, A.F.; Varma, M.V.; Steyn, S.J.; Scott, D.O.; Maurer, T.S.; Bergman, A. Projecting ADME Behavior and Drug-Drug Interactions in Early Discovery and Development: Application of the Extended Clearance Classification System. *Pharm. Res.* **2016**, *33*, 3021–3030. [CrossRef]

Disclaimer/Publisher's Note: The statements, opinions and data contained in all publications are solely those of the individual author(s) and contributor(s) and not of MDPI and/or the editor(s). MDPI and/or the editor(s) disclaim responsibility for any injury to people or property resulting from any ideas, methods, instructions or products referred to in the content.